Cancer Management and Research

Dovepress

open access to scientific and medical research

Open Access Full Text Article

ORIGINAL RESEARCH

Circ-ZNF609 Accelerates the Radioresistance of Prostate Cancer Cells by Promoting the Glycolytic Metabolism Through miR-501-3p/HK2 Axis

This article was published in the following Dove Press journal:
Cancer Management and Research

Shuangkuan Du[1]
Pengjie Zhang[2]
Wei Ren[1]
Fan Yang[1]
Chun Du[1]

[1]Department of Urology, Shaanxi Provincial People's Hospital, Xi'an, Shaanxi 710068, People's Republic of China; [2]The Center of Kidney Diseases and Hemodialysis, Shaanxi Provincial People's Hospital, Xi'an, Shaanxi 710068, People's Republic of China

Background: The development of radioresistance remains the obstacle for prostate cancer (PCa) treatment. Here, we explored the role and potential mechanism of circular RNA zinc finger protein 609 (circ-ZNF609) in the radioresistance of PCa cells.

Materials and Methods: Quantitative real-time polymerase chain reaction (qRT-PCR) was used to detect the expression of circ-ZNF609, microRNA-501-3p (miR-501-3p) and hexokinase 2 (HK2) messenger RNA (mRNA). The viability, apoptosis, metastasis and radioresistance of PCa cells were assessed by 3-(4,5-dimethylthiazol-2-yl)-2,5-diphenyltetrazolium bromide (MTT) assay, flow cytometry, transwell assays and colony formation assay. The glycolytic rate was assessed through measuring the glucose consumption and lactate production using fluorescence-based glucose and lactate assay kits. The target interaction between miR-501-3p and circ-ZNF609 or HK2 was predicted by StarBase software and confirmed by dual-luciferase reporter assay and RNA immunoprecipitation (RIP) assay. The protein level of HK2 was detected by Western blot assay. In vivo tumor growth assay was used to explore the role of circ-ZNF609 in the radioresistance of PCa in vivo.

Results: Circ-ZNF609 was abnormally up-regulated in PCa tissues and cell lines. Circ-ZNF609 silencing hampered the viability, metastasis, radioresistance and promoted the apoptosis through suppressing cell glycolysis. MiR-501-3p was a direct target of circ-ZNF609, and si-circ-ZNF609-induced influence in PCa cells was partly alleviated by the addition of anti-miR-501-3p. MiR-501-3p functioned through directly interacting with and down-regulating HK2. HK2 was modulated by circ-ZNF609/miR-501-3p axis in PCa cells. Circ-ZNF609 silencing enhanced the radiosensitivity of PCa cells in vivo.

Conclusion: Circ-ZNF609 promoted the progression and radioresistance of PCa cells through accelerating the glycolysis via miR-501-3p/HK2 axis, providing promising targets for improving the prognosis of PCa patients.

Keywords: prostate cancer, circ-ZNF609, miR-501-3p, HK2, glycolysis, radioresistance

Introduction

Prostate cancer (PCa) is a common malignancy in males.[1] Radiation and radical prostatectomy are important therapeutic strategies for PCa patients.[2] However, the relapse and metastasis of high-risk PCa patients limit the therapeutic effect of radiation.[3] Understanding the molecular mechanism of radioresistance of PCa cells is needed to treat high-risk PCa patients.

Warburg effect is one of the hallmarks of cancers that featured by altered glycolytic metabolism.[4,5] Tumor cells convert glucose into lactate to extract energy

Correspondence: Pengjie Zhang
Email ls6uhp@163.com

submit your manuscript | www.dovepress.com
DovePress
http://doi.org/10.2147/CMAR.S257441

under aerobic condition.[6] Warburg effect promotes the metastasis and inhibits the apoptosis of cancer cells.[7,8] In this study, we uncovered the internal link between the radioresistance and the glycolytic metabolism of PCa cells.

Circular RNAs (circRNAs) are a class of non-coding RNAs (ncRNAs) that characterized by the loop structure.[9] Due to their stable loop structure and differential expression in tumor cells and normal cells, circRNAs are ideal diagnostic and prognostic markers for cancers.[10] The level of circ-zinc finger protein 609 (circ-ZNF609) was higher in PCa, and circ-ZNF609 promoted the malignant behaviors of PCa cells through sponging microRNA-186-5p (miR-186-5p).[11] We aimed to clarify the association between the abundance of circ-ZNF609 and the radioresistance in PCa cells.

MicroRNAs (miRNAs) are another class of ncRNAs with about 22 nucleotides.[12] Emerging evidence pointed out the vital functions of miRNAs in many cancers.[13,14] The anti-tumor role of miR-501-3p was verified in non-small cell lung cancer (NSCLC), hepatocellular carcinoma and PCa.[15–17] MiR-501-3p hampered the progression of PCa through regulating CREPT/cyclin D1 signaling.[17] However, the role of miR-501-3p in the radioresistance and glycolysis of PCa cells remains to be uncovered.

Hexokinase 2 (HK2) is one of the key enzymes in glycolysis. He et al found that HK2 was up-regulated in cisplatin-resistant NSCLC cells compared with parental cells.[18] Cao et al claimed that circ-RNF20 accelerated the progression and glycolysis of breast cancer cells through regulating miR-487a/HIF-1α/HK2 axis.[19] The expression pattern and working mechanism of HK2 in PCa were investigated in this study.

We initially assessed the expression profile of circ-ZNF609 in PCa tissues and adjacent normal tissues. The roles of circ-ZNF609 in the cell viability, apoptosis, metastasis, radioresistance and aerobic glycolysis were explored. Subsequently, we uncovered the molecular mechanism behind circ-ZNF609-mediated influence in PCa.

Materials and Methods

Tissue Samples and Ethical Statement

A total of 30 pairs of PCa tissues and corresponding normal tissues were collected from 30 PCa patients in Shaanxi Provincial People's Hospital. Informed consents were provided from each participant before enrollment. The protocol in this clinical study was authorized by the Ethics Committee of Shaanxi Provincial People's Hospital. qRT-PCR was applied to detect the expression of circ-ZNF609, miR-501-3p and HK2 in these tumor tissues and adjacent normal tissues. Clinicopathological features of prostate cancer patients are listed in Table 1.

Cell Culture, Chemical and Transfection

PCa cell lines (22Rv1, LNCaP, DU145 and VCaP) and normal human prostate epithelial cell line (RWPE-1) were purchased from BeNa Culture Collection (Beijing, China). Cells were routinely cultured in Roswell Park Memorial Institute-1640 (RPMI-1640) medium (Gibco, Carlsbad, CA, USA) added with 10% fetal bovine serum (FBS; Biowest, Loire Valley, France), 10% penicillin (100 U/mL) and 10% streptomycin (100 μg/mL) at a 37°C incubator with 5% CO_2.

2-Deoxy-D-glucose (2-DG) acts as a glycolytic inhibitor with antiviral activity, and it was purchased from Selleck (Shanghai, China).

For circ-ZNF609 knockdown, small interfering RNA targeting circ-ZNF609 (si-circ-ZNF609) and short hairpin RNA targeting circ-ZNF609 (sh-circ-ZNF609) were used, and siRNA negative control (si-NC) and shRNA-NC (sh-NC) acted as the controls. For the overexpression and knockdown of miR-501-3p, miR-501-3p mimics (miR-501-3p) and miR-501-3p inhibitor (anti-miR-501-3p) were used, and miRNA-NC (miR-NC) and anti-miR-NC were used as controls. For the overexpression of HK2 and circ-ZNF609, HK2 and circ-ZNF609 overexpression plasmid (HK2 and circ-ZNF609) were used, and pcDNA was used as the control. These oligonucleotides and plasmids were purchased from Genepharma (Shanghai, China). Lipofectamine 3000 (Invitrogen, Paisley Scotland, UK) was used for transfection manipulation.

X-Ray Irradiation

X-ray generator (Varian, Palo Alto, CA, USA) was used for the administration of radiation with the fixed rate of 4 Gy/min.

Table 1 Clinicopathological Features of Prostate Cancer Patients

Clinicopathological Features (n=30)		
Age	>55 ≤55	21 9
Tumor stage	I–II III–IV	19 11
Metastasis	Negative Positive	17 13

Quantitative Real-Time Polymerase Chain Reaction (qRT-PCR)

The isolation of RNA sample was conducted with TRIzol reagent (Invitrogen). The purity and concentration of RNA samples were analyzed using Agilent 2100 Bioanalyzer (Agilent Technologies, Santa Clara, CA, USA). To measure the expression of circ-ZNF609 and HK2, 1 μg RNA was reversely transcribed into complementary DNA (cDNA) with the Bio-Rad iScript kit (Bio-Rad, Hercules, CA, USA), and the amplification was conducted using iQSYBR Green SuperMix (Bio-Rad). Glyceraldehyde-3-phosphate dehydrogenase (GAPDH) served as the internal reference for circ-ZNF609 and HK2. To detect the level of miR-501-3p, TaqMan reverse transcription kit (Applied Biosystems, Rotkreuz, Switzerland) and TaqMan MicroRNA assay kit (Applied Biosystems) were used. U6 acted as the internal control for miR-501-3p. The primers used in this study were listed in Table 2. The expression of circ-ZNF609, miR-501-3p and HK2 was analyzed using the 2-ΔΔCt method.

3-(4,5-Dimethylthiazol-2-Yl)-2,5-Diphenyltetrazolium Bromide (MTT) Assay

PCa cells were plated into the wells of 96-well plates (1×10^3 cells/well; n=6). After transfecting for 72 h, DU145 and VCaP cells were incubated with 10 μL MTT (Invitrogen) for 4 h. A total of 200 μL dimethylsulfoxide (DMSO; Sangon Biotech, Shanghai, China) was added to dissolve the formazan crystals. The quantification of formazan crystals was measured at 490 nm to indicate the number of viable PCa cells. This experiment was repeated for three times.

Table 2 Primers in qRT-PCR Assay

Gene Name	Primer Sequence
circ-ZNF609	TGAGTGTCGCCTGCTAAAGA (forward; F) CCCCCAGCTTTCCTATTTTC (reverse; R)
miR-501-3p	AATGCACCCGGGCAAGGATTCT (F) AGAATCCTTGCCCGGGTGCATT (R)
HK2	CTTCTTCACGGAGCTCAACC (F) AAGCCCTTTCTCCATCTCCT (R)
U6	GCTTCGGCAGCACATATACT (F) GTGCAGGGTCCGAGGTATTC (R)
GAPDH	CTGGGCTACACTGAGCACC (F) AAGTGGTCGTTGAGGGCAATG (R)

Flow Cytometry

The apoptosis rate was calculated by an Annexin V-fluorescein isothiocyanate (FITC)/propidine iodide (PI) Apoptosis Kit (Bender Med System, Vienna, Austria). PCa cells were seeded in 6-well plates in triplicates at the concentration of 2×10^5 cells/well. After relevant transfection for 72 h, PCa cells were harvested using trypsin and rinsed three times using phosphate buffered saline (PBS) buffer. After re-suspending PCa cells with 200 μL binding buffer, 62.5 ng/mL Annexin V combined FITC and 5 μg/mL PI were added to probe the PCa cells in the dark for 15 min at 37°C. Cell apoptosis was analyzed by FC-500 flow cytometer (Beckman Coulter, Pasadena, CA, USA) using Beckman CXP software, and three technical repetitions were conducted in one sample. The apoptosis rate indicated the apoptotic PCa cells in early stage ($FITC^+/PI^-$) and late stage ($FITC^+/PI^+$). This experiment was repeated for three times.

Transwell Assays

Transwell plates with 8 μm inserts (Costar, Corning, NY, USA) were used in transwell migration assay. In transwell invasion assay, transwell plates and Matrigel-precoated inserts were used. After transfection for 24 h, PCa cells (1×10^4 cells in transwell migration assay and 8×10^4 cells in transwell invasion assay) were plated into the upper chambers in 200 μL serum-free medium (n=3), and the lower chambers were filled with culture medium with 10% FBS. After 24-h incubation, the migrated or invaded PCa cells in five random fields were counted using an optical microscope. This experiment was repeated for three times.

Colony Formation Assay

Transfected PCa cells were irradiated with 0 Gy, 2 Gy, 4 Gy, 6 Gy or 8 Gy using X-ray generator (Varian) with the fixed rate of 4 Gy/min. These PCa cells were re-seeded into 6-well plates in triplicate at the density of 400 cells per well and cultured for 2 weeks. The culture medium was refreshed every 3 d. When the colonies were visible, the colonies were stained with 0.5% crystal violet (Wellbio, Shanghai, China) and counted under the light microscope. Survival fraction in each group was analyzed through normalizing the number of visible colonies in experimental groups to that in their corresponding Control group. This experiment was repeated for three times.

Glycolytic Metabolism Analysis

PCa cells were plated in 6-well plates in triplicates at the concentration of 1.5×10^5 cells/well. After culturing PCa cells in glucose-free medium for 16 h, the glucose-free medium was replaced by high glucose medium for 24 h. The rates of glucose consumption and lactate production were analyzed using fluorescence-based glucose and lactate assay kits (BioVision, Milpitas, California, USA). This experiment was repeated for three times.

Bioinformatic Prediction

StarBase database was utilized to analyze the interactions of circ-ZNF609-miRNAs and miR-501-3p-mRNAs.

Dual-Luciferase Reporter Assay

The fragments of circ-ZNF609 and HK2 messenger RNA (mRNA) containing the miR-501-3p binding sites were amplified by PCR and inserted into pmirGLO vector (Promega, Madison, WI, USA) with two enzymes (Nhel and Xbal), termed as wild-type (WT)-circ-ZNF609 and HK2 3′untranslated region (3′UTR)-WT. Meanwhile, the corresponding mutant fragments of circ-ZNF609 and HK2 mRNA harboring the mutant binding sites with miR-501-3p were also cloned into pmirGLO vector (Promega) to generate MUT-circ-ZNF609 and HK2 3′UTR-MUT with two enzymes (Nhel and Xbal). Sequence alignment was conducted using Bioxm software. PCa cells were seeded in 24-well plates at the density of 4×10^4 cells/well to settle down. Luciferase reporter plasmids (50 ng) were transfected into PCa cells with 20 nM miR-NC or miR-501-3p using Lipofectamine 3000 (Invitrogen). The luciferase activities of Firefly and Renilla were detected using Dual-luciferase reporter assay system kit (Promega) using luminometer (Plate Chameleon V, Hidex, Finland) after transfection for 48 h. Firefly luciferase intensity was normalized to Renilla fluorescence intensity. This experiment was repeated for three times.

RNA Immunoprecipitation (RIP) Assay

Magna RNA immunoprecipitation kit (Millipore, Bedford, MA, USA) was used to conduct RIP assay. PCa cells were seeded in 6 cm culture plate at the density of 5×10^5 cells/plate. After collecting and disrupting using ice-cold Radioimmunoprecipitation (RIPA) lysis buffer (Beyotime, Shanghai, China). Anti-Argonaute 2 (anti-Ago2) or anti-Immunoglobulin G (anti-IgG) was incubated with cell lysate for 4 h. Subsequently, protein A/G beads were added to incubate for a further 2 h. qRT-PCR was used to detect the expression of circ-ZNF609, miR-501-3p and HK2 mRNA. This experiment was repeated for three times.

Western Blot Assay

After transfection for 24 h, PCa cells were harvested using PBS and then disrupted using cell lysis buffer (Abcam, Cambridge, MA, USA) for 30 min. Cell debris was removed through high-speed centrifugation. Protein quantification was conducted using BCA assay kit (Bio-Rad). An equal amount of protein samples (25 μg) were subjected to sodium dodecyl sulfate polyacrylamide gel electrophoresis (SDS-PAGE) gel and electro-transferred onto a polyvinylidene fluoride (PVDF) membrane (Millipore). The membrane was blocked with 5% skim milk for 1 h, and then the membrane was incubated with primary antibodies at 4°C overnight. Horseradish peroxidase (HRP)-conjugated anti-rabbit IgG was used to incubate the membrane for 2 h. The protein signals were visualized with enhanced chemiluminescence (ECL) reagent (GE Healthcare, Piscataway, NJ, USA) and several X-ray films. The primary antibodies used in this study were listed as followed: anti-HK2 (ab209847; Abcam) and anti-GAPDH (ab181602; Abcam). ImageJ software was used for gray analysis. This experiment was repeated for three times.

In vivo Tumor Growth Assay

The study protocol was authorized by the Animal Research Committee of Shaanxi Provincial People's Hospital. Animal studies were performed in compliance with the ARRIVE guidelines and the Basel Declaration. All animals received humane care according to the National Institutes of Health (USA) guidelines. A total of 28 BALB/c nude mice (five-week-old) were purchased from Guangdong Medical Laboratory Animal Center (Foshan, China) to construct the xenograft model. DU145 cells (4×10^6 cells/200 μL PBS) stably transfected with sh-NC or sh-circ-ZNF609 were subcutaneously injected to the right flanks of the nude mice, and mice in sh-NC group and sh-circ-ZNF609 group were randomly divided into non-irradiation group and irradiation group. After 8-d injection, the tumor area of the mice in irradiation group was irradiated with 4 Gy every 4 d using X-ray generator (Varian) with the fixed rate of 4 Gy/min. The volume of tumors was monitored every 4 d by length × width^2 × 0.5. After 28-d injection, the tumors were resected and the weight was recorded. The level of circ-ZNF609 was examined by qRT-PCR.

Statistical Analysis

The statistical data from three independent experiments were represented as mean ± standard deviation (SD). Comparisons were analyzed using Student's *t*-test for normally distributed experimental data in two groups and one-way ANOVA followed by Tukey's test among multiple groups. Linear relationship was analyzed using Spearman correlation coefficient. Value of $P < 0.05$ was considered statistical significance.

Results

Circ-ZNF609 is Highly Expressed in PCa

The level of circ-ZNF609 was detected in PCa tissues and cells by qRT-PCR. The results revealed that circ-ZNF609 was highly expressed in PCa tissues and cell lines compared with adjacent non-tumor tissues and normal human prostate epithelial cell line RWPE-1 (Figure 1A and B).

Circ-ZNF609 Silencing Inhibits the Progression and Radioresistance of PCa in vitro

To investigate the functions of circ-ZNF609 in PCa cells, we carried out loss-of-function experiments. The level of circ-ZNF609 in PCa cells was decreased when we transfected si-circ-ZNF609 (Figure 2A), and this result demonstrated that the knockdown efficiency of si-circ-ZNF609 was high. Subsequently, we explored the effects of circ-ZNF609 silencing on the viability, apoptosis, metastasis, glycolysis and radioresistance of PCa cells. After transfection for 72 h, the viability of PCa cells was notably reduced with the silencing of circ-ZNF609 (Figure 2B and C). Circ-ZNF609 silencing induced the apoptosis of PCa cells (Figure 2D). Transwell assays were conducted to measure the migrated and invaded PCa cells in different groups to analyze the influence of circ-ZNF609 silencing on the metastasis of PCa cells. The abilities of migration and invasion were significantly suppressed with the interference of circ-ZNF609 (Figure 2E and F). PCa cells transfected with si-NC or si-circ-ZNF609 were irradiated with different doses to test the effect of circ-ZNF609 silencing on the radioresistance of PCa cells. The survival fraction was prominently reduced with the interference of circ-ZNF609 (Figure 2G and H). Warburg effect is an important hallmark for cancers. We assessed the glycolytic metabolism of PCa cells through measuring glucose consumption and lactate production. Circ-ZNF609 interference suppressed the uptake of glucose and the production of lactate (Figure 2I and J). The overexpression efficiency of circ-ZNF609 was high in PCa cells (Figure 2K). 2-DG is an inhibitor of glycolysis. As mentioned in Figure 2L and M, circ-ZNF609 overexpression elevated the radioresistance of PCa cells, and the addition of 2-DG remarkably suppressed the radioresistance of PCa cells, suggested that circ-ZNF609 elevated the radioresistance of PCa cells through promoting glycolysis. In summary, circ-ZNF609 promoted the radioresistance of PCa cells through enhancing the glycolysis.

Circ-ZNF609 Directly Interacts with miR-501-3p

We performed bioinformatic software StarBase to search the direct downstream targets of circ-ZNF609 to reveal the molecular mechanism of circ-ZNF609 in the viability, apoptosis, metastasis, glycolysis and radioresistance of PCa cells. MiR-501-3p was predicted as a possible target of circ-ZNF609 (Figure 3A). Luciferase reporter plasmids were constructed through inserting the wild-type or mutant-type binding sequence with miR-501-3p in circ-ZNF609 into reporter vectors. DU145 and VCaP cells were co-transfected with

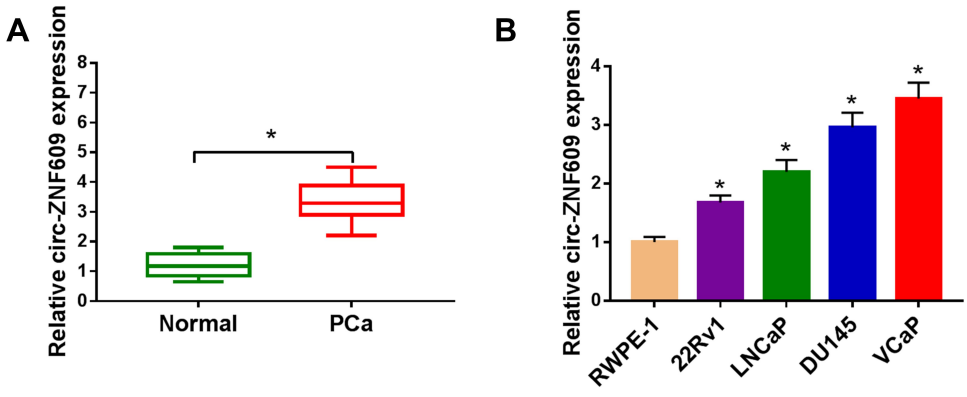

Figure 1 Circ-ZNF609 is highly expressed in PCa. (**A**) The level of circ-ZNF609 was examined in PCa tissues and matching non-tumor tissues by qRT-PCR. (**B**) qRT-PCR was applied to detect the level of circ-ZNF609 in normal human prostate epithelial cell line and a panel of four PCa cell lines. *P<0.05.

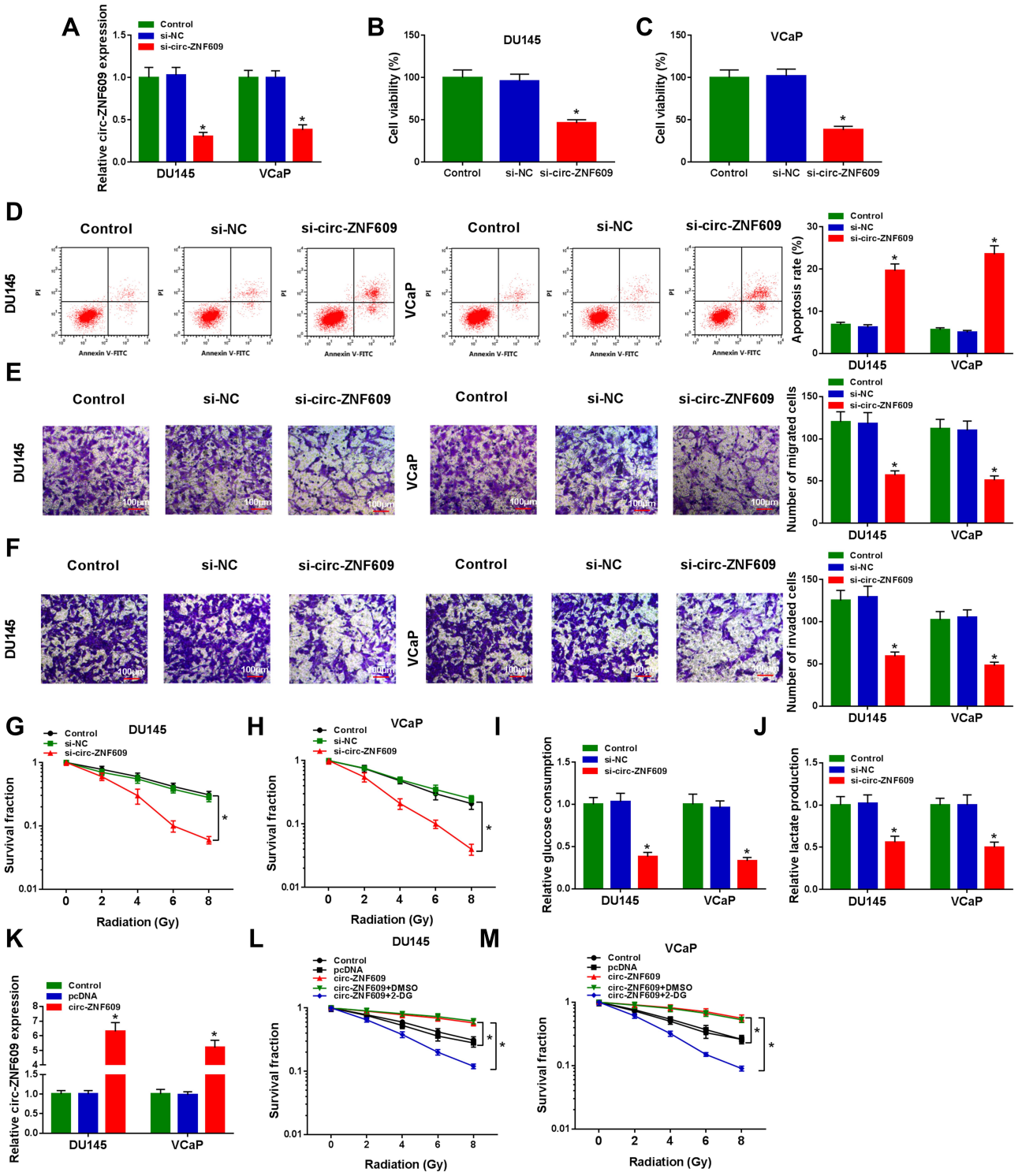

Figure 2 Circ-ZNF609 silencing inhibits the progression and radioresistance of PCa in vitro. (**A**–**K**) DU145 and VCaP cells were transfected with 300 nM si-NC or si-circ-ZNF609, respectively. (**A**) The relative expression of circ-ZNF609 was detected in PCa cells by qRT-PCR after transfection for 48 h. (**B** and **C**) The viability of PCa cells was analyzed by MTT assay after transfection for 72 h. (**D**) Flow cytometry was used to detect the apoptosis rate of PCa cells in Control group, si-NC transfected group and si-circ-ZNF609 transfected group after transfection for 72 h. (**E** and **F**) Transwell assays were conducted to assess the migration and invasion abilities of PCa cells in Control, si-NC and si-circ-ZNF609 groups after transfection for 24 h. (**G** and **H**) Colony formation assay was used to evaluate the radioresistance of PCa cells in different groups with increased doses of irradiation (2 Gy, 4 Gy, 6 Gy and 8 Gy). (**I** and **J**) Fluorescence-based glucose and lactate assay kits were used to detect the glycolytic metabolism rate of PCa cells. (**K**) The level of circ-ZNF609 was examined in DU145 and VCaP cells transfected with 1 μg pcDNA or circ-ZNF609 plasmid by qRT-PCR. (**L** and **M**) DU145 and VCaP cells were treated with pcDNA, circ-ZNF609, circ-ZNF609 + DMSO or circ-ZNF609 + 2-DG. The radioresistance of PCa cells was assessed by colony formation assay. *P<0.05.

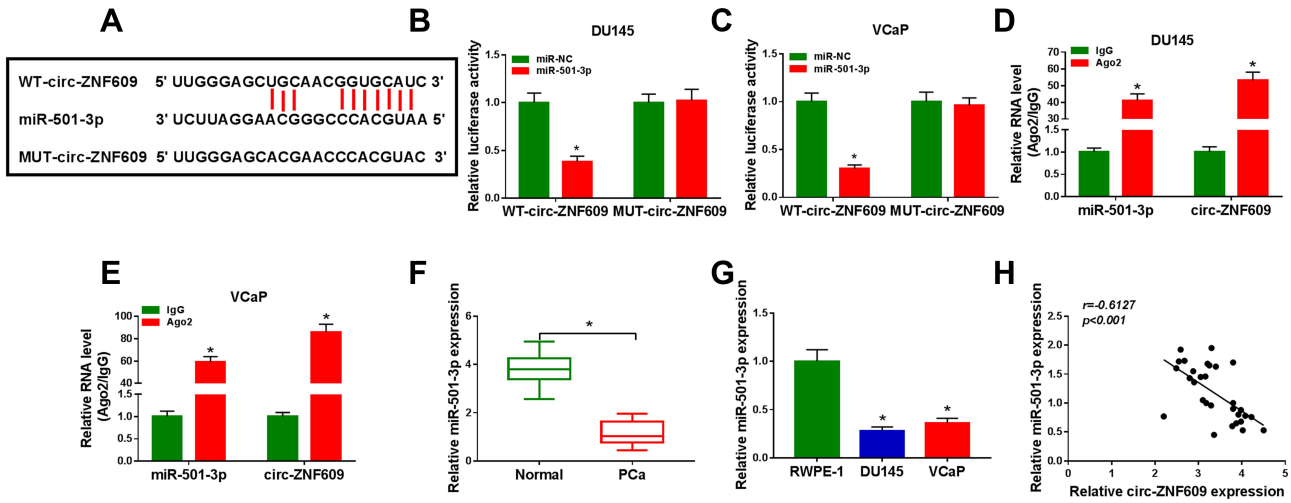

Figure 3 Circ-ZNF609 directly interacts with miR-501-3p. (**A**) The potential binding region with miR-501-3p in circ-ZNF609 (predicted by StarBase software) and the mutant form of circ-ZNF609 were shown. (**B** and **C**) The target interaction between circ-ZNF609 and miR-501-3p was analyzed by dual-luciferase reporter assay. (**D** and **E**) RIP assay was used to test whether miR-501-3p could bind to circ-ZNF609 in PCa cells. (**F** and **G**) The expression of miR-501-3p was examined in PCa tissues and cells along with adjacent normal tissues and RWPE-1 cells by qRT-PCR. (**H**) Spearman correlation coefficient was used to analyze the correlation between the expression of miR-501-3p and circ-ZNF609 in PCa tissues. *P<0.05.

these re-constructed reporter plasmids and miR-NC or miR-501-3p. MiR-501-3p accumulation notably down-regulated the luciferase activity in WT-circ-ZNF609 group in comparison with MUT-circ-ZNF609 group (Figure 3B and C), manifested that miR-501-3p directly interacted with circ-ZNF609 through the predicted binding sites. MiRNAs are generally known to form Ago2-contained RNA-induced silencing complex (RISC).[20] Therefore, we investigated the spatial interaction between miR-501-3p and circ-ZNF609 in RISC through conducting RIP assay. Circ-ZNF609 and miR-501-3p were all substantially enriched in Ago2 group (Figure 3D and E), suggested that miR-501-3p interacted with circ-ZNF609. The expression pattern of miR-501-3p was also explored. MiR-501-3p was notably decreased in PCa tissues and cell lines in comparison with that in matching normal tissues and RWPE-1 cell line (Figure 3F and G). Through using Spearman correlation coefficient, we found that there was a negative correlation between miR-501-3p and circ-ZNF609 in PCa tissues (Figure 3H). These results together demonstrated that miR-501-3p was a direct target of circ-ZNF609 in PCa cells.

Circ-ZNF609 Modulates the Malignant Potential of PCa Cells Through Sponging miR-501-3p

We co-transfected si-circ-ZNF609 and anti-miR-501-3p into PCa cells. Si-circ-ZNF609 transfection elevated the expression of miR-501-3p, and the introduction of anti-miR-501-3p decreased the expression of miR-501-3p (Figure 4A). Si-circ-ZNF609-mediated suppressive effect on the viability of PCa cells was partly abated by the silencing of miR-501-3p (Figure 4B and C). The apoptosis was induced by si-circ-ZNF609, and the addition of anti-miR-501-3p partly alleviated the above promoting effect (Figure 4D). Si-circ-ZNF609 transfection also led to significant suppression on the migration (Figure 4E), invasion (Figure 4F), radioresistance (Figure 4G and H) and glycolysis (Figure 4I and J) of PCa cells. Nevertheless, these influences were attenuated by the co-transfection of anti-miR-501-3p in PCa cells (Figure 4E–J). We also explored if miR-501-3p regulated the radioresistance of PCa cells through modulating the glycolytic metabolism. Anti-miR-501-3p-mediated promotion on the glycolysis was notably suppressed by the treatment of 2-DG (Figure 4K and L). These results manifested that circ-ZNF609 promoted the radioresistance of PCa cells through promoting glycolysis via down-regulating miR-501-3p.

HK2 is a Direct Target of miR-501-3p

We conducted bioinformatic analysis (StarBase) to find the interacted genes of miR-501-3p. As mentioned in Figure 5A, HK2 was predicted as a target of miR-501-3p. MiR-501-3p transfection in HK2 3′UTR-WT group produced a lower luciferase activity (Figure 5B and C). Meanwhile, to test if the predicted binding sites with miR-501-3p in HK2 were essential for the combination between HK2 and miR-501-3p, we mutated the binding sites in HK2 to construct HK2 3′UTR-MUT reporter plasmid. The luciferase activity was

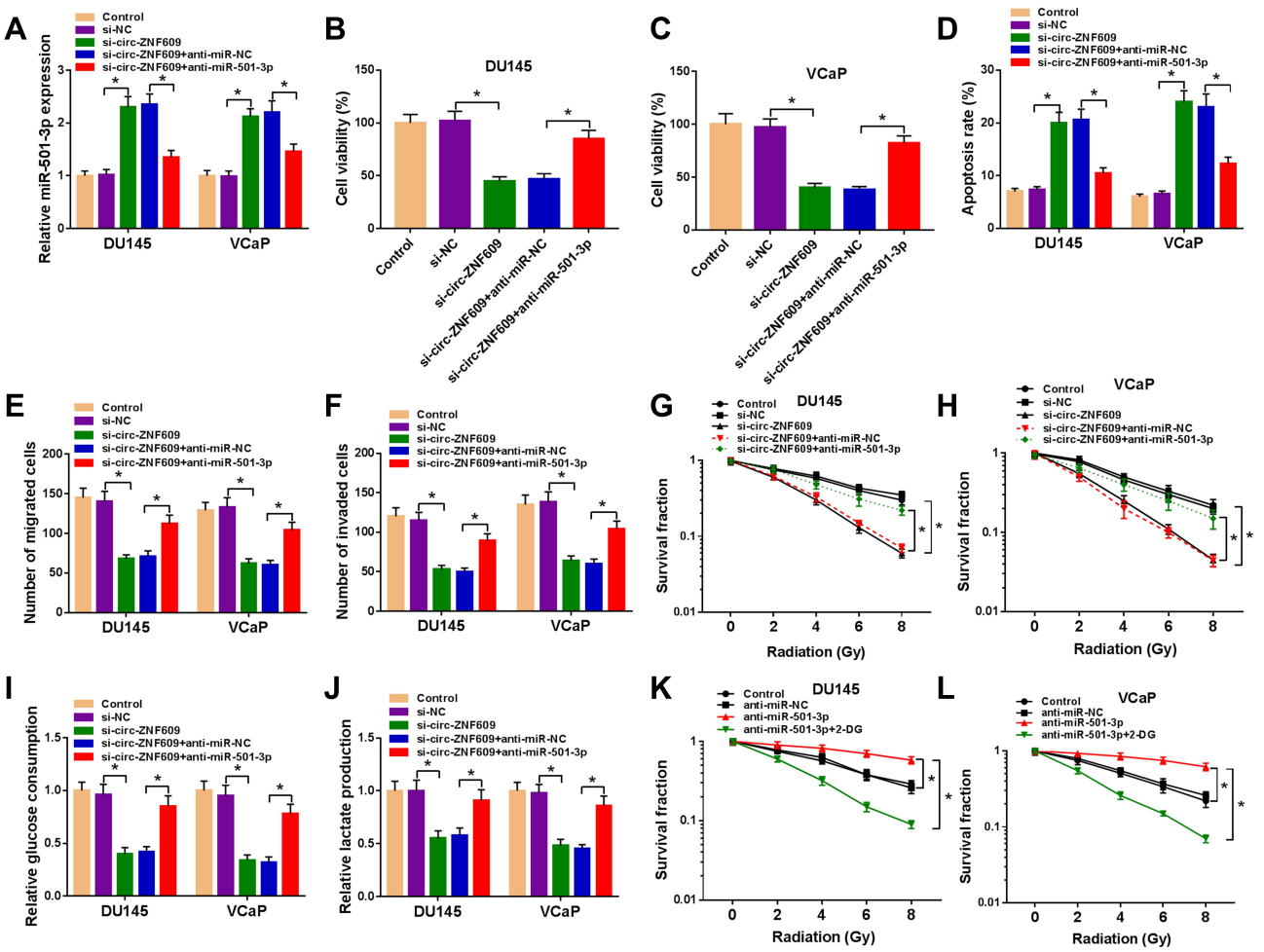

Figure 4 Circ-ZNF609 modulates the malignant potential of PCa cells through sponging miR-501-3p. (**A**–**J**) DU145 and VCaP cells were transfected with si-NC (300 nM), si-circ-ZNF609 (300 nM), si-circ-ZNF609 (300 nM) + anti-miR-NC (400 nM) or si-circ-ZNF609 (300 nM) + anti-miR-501-3p (400 nM). (**A**) The expression of miR-501-3p was detected in PCa cells by qRT-PCR after transfection for 48 h. (**B** and **C**) Cell viability of PCa cells was analyzed using MTT assay after transfection for 72 h. (**D**) Flow cytometry was used to analyze the apoptosis rate of transfected PCa cells after transfection for 72 h. (**E** and **F**) The migration and invasion capacities of PCa cells were analyzed through transwell assays after transfection for 24 h. (**G** and **H**) The radioresistance of PCa cells was assessed through measuring survival fraction using colony formation assay. (**I** and **J**) The influence of circ-ZNF609 and miR-501-3p in the glycolysis of PCa cells was evaluated using fluorescence-based glucose and lactate assay kits. (**K** and **L**) PCa cells were treated with anti-miR-NC, anti-miR-501-3p or anti-miR-501-3p + 2-DG, and colony formation assay was used to analyze the radioresistance of DU145 and VCaP cells with various doses of irradiation. *P<0.05.

unaffected in HK2 3′UTR-MUT group when co-transfected with miR-NC or miR-501-3p (Figure 5B and C) suggested that miR-501-3p directly interacted with HK2 mRNA through the predicted sites in PCa cells. The results of RIP assay also revealed that miR-501-3p could bind to HK2 mRNA (Figure 5D and E). The expression of HK2 in PCa tissues, normal tissues, PCa cell lines and normal human prostate epithelial cell line was measured by qRT-PCR and Western blot assay. The mRNA and protein levels of HK2 were conspicuously up-regulated in PCa tissues compared with that in adjacent normal tissues (Figure 5F and G). Also, both the mRNA and protein expression of HK2 was higher in PCa cells in comparison with that in RWPE-1 cells (Figure 5I and J). Through analyzing the expression of HK2 and miR-501-3p in PCa tissues, we found that there was a negative correlation between the expression of HK2 and miR-501-3p (Figure 5H). In summary, miR-501-3p directly interacted with HK2 mRNA in PCa cells.

MiR-501-3p Functions Through Targeting HK2 in PCa

We co-transfected miR-501-3p and HK2 into PCa cells to explore if miR-501-3p functioned through targeting HK2. MiR-501-3p overexpression down-regulated the protein expression of HK2, and the addition of HK2 plasmid recovered the expression of HK2 (Figure 6A). The viability of PCa cells was decreased with the accumulation of miR-501-3p, the co-transfection of miR-501-3p and HK2

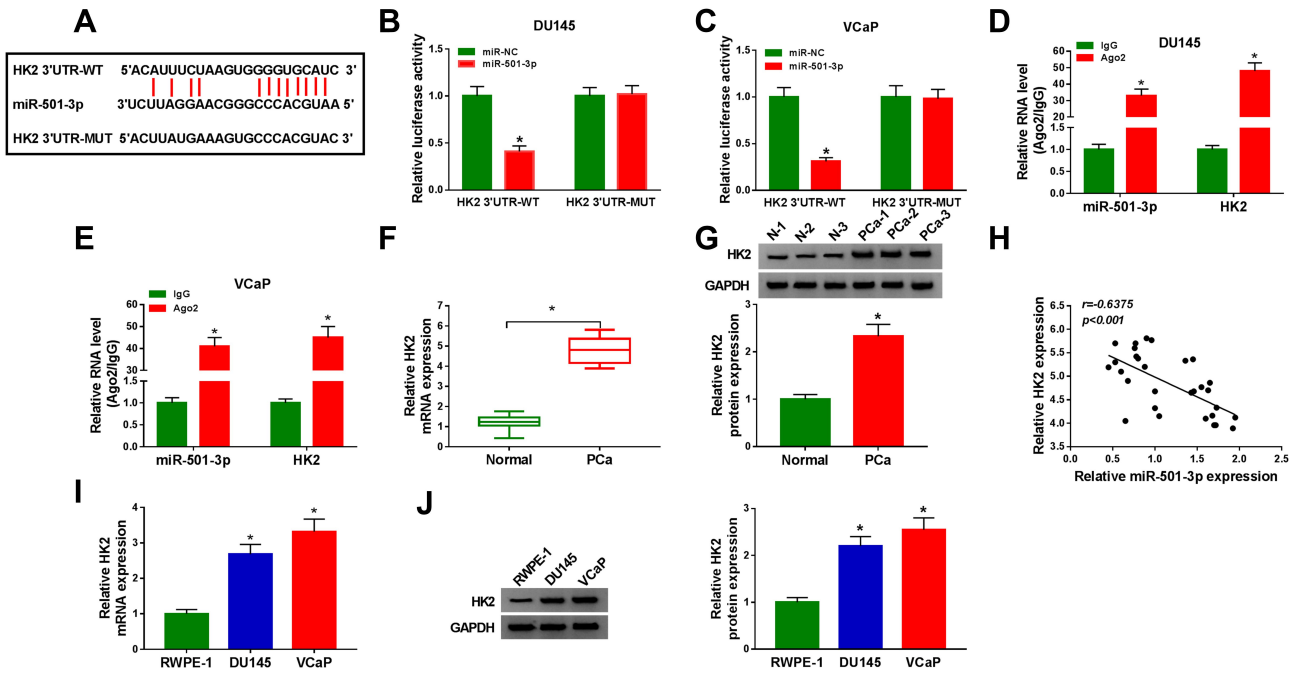

Figure 5 HK2 is a direct target of miR-501-3p. (**A**) The binding region between HK2 and miR-501-3p was predicted by StarBase dataset. The mutant-type of HK2 sequence was also shown. (**B** and **C**) The target interaction between miR-501-3p and HK2 was measured by dual-luciferase reporter assay. (**D** and **E**) RIP assay was utilized to assess the combination between miR-501-3p and HK2. (**F** and **G**) The mRNA and protein levels of HK2 were detected by qRT-PCR and Western blot assay. (**H**) The linear relationship between the expression of miR-501-3p and HK2 was analyzed by Spearman correlation coefficient. (**I** and **J**) qRT-PCR and Western blot assay were used to detect the mRNA and protein expression of HK2 in PCa cells and RWPE-1 cells. *P<0.05.

rescued the viability of PCa cells (Figure 6B and C). MiR-501-3p-mediated promotion on the apoptosis and inhibition of the migration and invasion of PCa cells were partly alleviated by the co-transfection of miR-501-3p and HK2 (Figure 6D–F). MiR-501-3p transfection suppressed the radioresistance and glycolysis of PCa cells, and the addition of HK2 recovered the glycolytic metabolism and radioresistance of PCa cells (Figure 6G–J). HK2 accumulation elevated the radioresistance of PCa cells, and the addition of glycolysis inhibitor (2-DG) blocked the radioresistance of PCa cells (Figure 6K and L). Taken together, miR-501-3p inhibited the radioresistance of PCa cells through suppressing the glycolytic metabolism via HK2.

Circ-ZNF609 Up-Regulates HK2 Through Targeting miR-501-3p

In order to illustrate the regulatory relationship among circ-ZNF609, miR-501-3p and HK2, DU145 and VCaP cells were transfected with si-circ-ZNF609 alone or together with anti-miR-501-3p. Circ-ZNF609 silencing caused a distinct decrease in the protein expression of HK2, and this inhibitory effect was attenuated by the co-transfection of anti-miR-501-3p (Figure 7A and B). Overall, circ-ZNF609 enhanced the level of HK2 through sequestering miR-501-3p.

Circ-ZNF609 Silencing Elevates Radiosensitivity of PCa in vivo

Given the results that circ-ZNF609 promoted the radioresistance of PCa cells in vitro, we explored if circ-ZNF609 exerted a similar role in vivo. After injecting DU145 cells stably transfected with sh-circ-ZNF609 or sh-NC for 8 d, the mice in IR group were irradiated with 4 Gy every 4 d. The tumor volume was monitored every 4 d. At the end point, the tumor weight and the expression of circ-ZNF609 in tumor tissues were detected. Circ-ZNF609 expression was notably reduced in DU145 cell line stably transfected with sh-circ-ZNF609 compared with that stably transfected with sh-NC (Figure 8A). Circ-ZNF609 silencing alone or IR exposure alone significantly suppressed the growth of PCa tumors (Figure 8B and C). Furthermore, tumors were smaller in circ-ZNF609 silencing and IR group compared with IR group, suggested that circ-ZNF609 silencing enhanced the radiosensitivity of PCa cells in vivo (Figure 8B and C). The level of circ-ZNF609 was decreased in sh-circ-ZNF609 group and sh-NC + IR group compared with sh-NC group, and the level

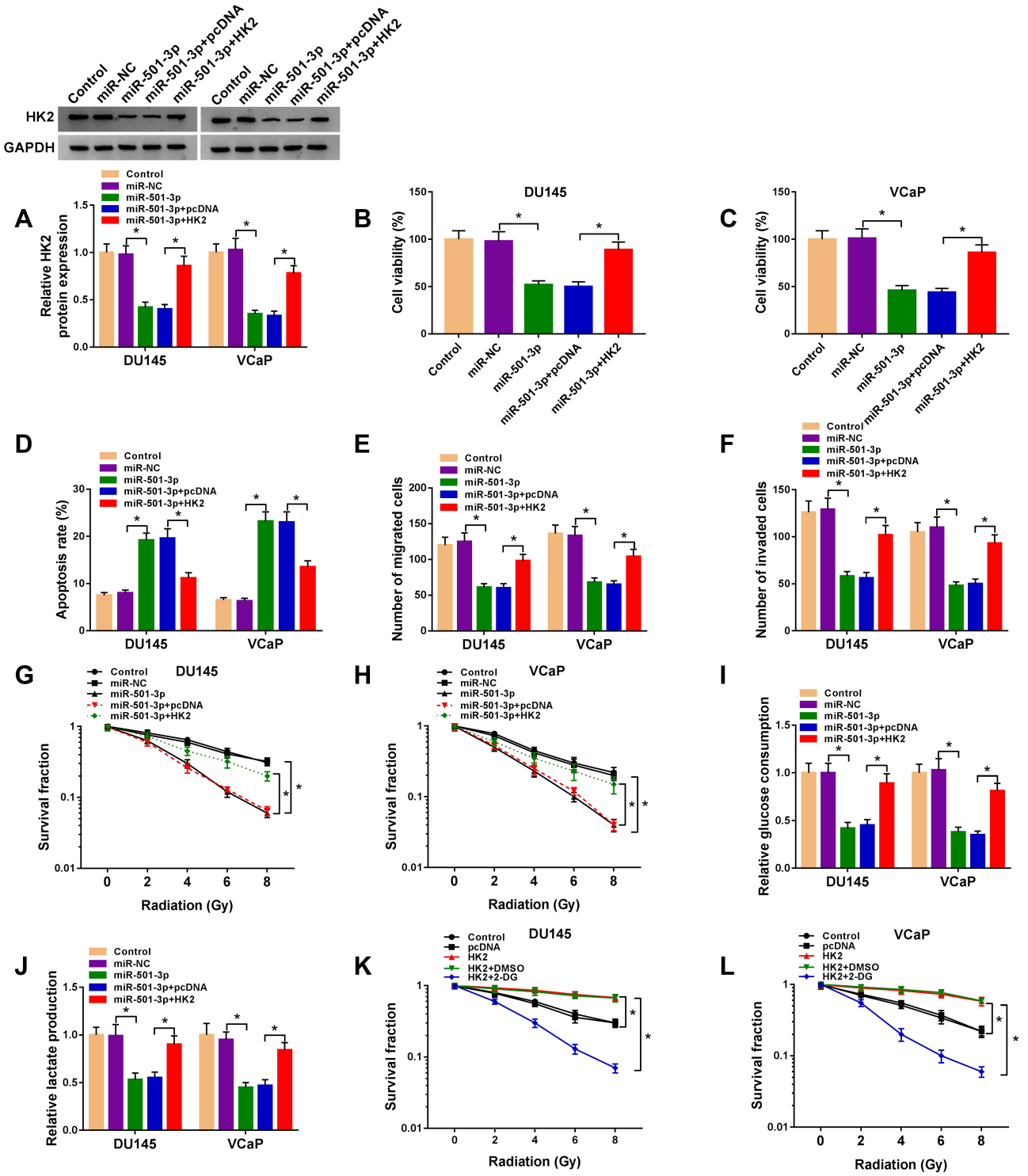

Figure 6 MiR-501-3p functions through targeting HK2 in PCa. (**A**–**J**) DU145 and VCaP cells were transfected with miR-NC (400 nM), miR-501-3p (400 nM), miR-501-3p (400 nM) + pcDNA (1 μg) or miR-501-3p (400 nM) + HK2 (1 μg). (**A**) The protein level of HK2 was examined in PCa cells by Western blot assay after transfection for 48 h. (**B** and **C**) MTT assay was used to examine the cell viability of PCa cells after transfection for 72 h. (**D**) The apoptosis of transfected PCa cells was assessed by flow cytometry after transfection for 72 h. (**E** and **F**) The migration and invasion of PCa cells were analyzed by Transwell assays after transfection for 24 h. (**G** and **H**) Colony formation assay was used to assess the radioresistance of PCa cells. (**I** and **J**) The glucose consumption and lactate production were measured to analyze the glycolysis of PCa cells with fluorescence-based glucose and lactate assay kits. (**K** and **L**) DU145 and VCaP cells were treated with pcDNA, HK2 plasmid or HK2 plasmid and 2-DG. Colony formation assay was used to analyze the radioresistance of PCa cells. *P<0.05.

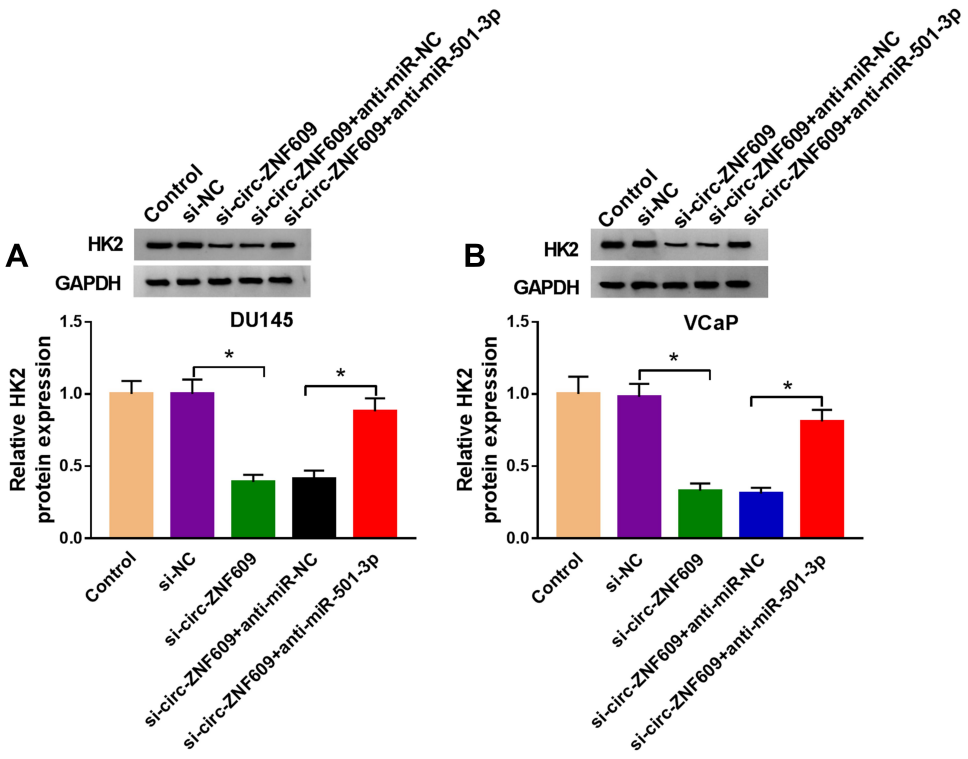

Figure 7 Circ-ZNF609 up-regulates HK2 through targeting miR-501-3p. (**A** and **B**) DU145 and VCaP cells were transfected with si-NC (300 nM), si-circ-ZNF609 (300 nM), si-circ-ZNF609 (300 nM) + anti-miR-NC (400 nM) or si-circ-ZNF609 (300 nM) + anti-miR-501-3p (400 nM). The expression of HK2 was analyzed by Western blot assay after transfection for 48 h. *P<0.05.

of circ-ZNF609 was further reduced in sh-circ-ZNF609 + IR group than that in sh-NC + IR group (Figure 8D). In summary, circ-ZNF609 elevated radioresistance of PCa cells in vivo.

Discussion

CircRNAs have been emerged as pivotal regulators in the initiation and progression of many malignancies.[21,22] Circ_102171 accelerated the development of papillary thyroid cancer through modulating CTNNBIP1/β-catenin signaling.[23] Circ_100269 inhibited the growth of gastric cancer cells through targeting miR-630.[24] In this study, circ-ZNF609 was found to be overexpressed in PCa tissues and cells compared with adjacent normal tissues and RWPE-1 cells. Radioresistance is the obstacle for PCa treatment. Furthermore, aerobic glycolysis is a hallmark of cancers, and it provides the advantage for the proliferation of cancer cells.[6] The association among the dysregulation of circRNAs, the development of radioresistance and the promotion in glycolysis has been reported before. For instance, circPITX1 silencing elevated the radiosensitivity of glioma cells through suppressing the glycolysis by regulating miR-329-3p/NEK2 axis.[25] Loss-of-function experiments were employed to explore the functions of circ-ZNF609 in PCa cells. Circ-ZNF609 knockdown caused the suppression of the viability, migration and invasion and the promotion on the apoptosis of PCa cells. The role of circ-ZNF609 in PCa cells was in agreement with the former article.[11] Furthermore, circ-ZNF609 silencing enhanced the radiosensitivity and inhibited the glycolytic metabolism rate of PCa cells. We investigated if circ-ZNF609 silencing-mediated up-regulation in the radiosensitivity was due to the suppression of glycolysis, and 2-DG (inhibitor of glycolysis) was used in further experiments. Circ-ZNF609 overexpression promoted the radioresistance of PCa cells, and this promoting effect was remarkably attenuated by the addition of 2-DG, demonstrated that circ-ZNF609 promoted the radioresistance of PCa cells through accelerating the glycolysis.

To disclose the crucial molecules involved in circ-ZNF609-mediated regulation of PCa cells, bioinformatic software (StarBase) was used. MiR-501-3p was predicted as a possible target of circ-ZNF609 by StarBase software. The target interaction between miR-501-3p and circ-ZNF609 was verified using dual-luciferase reporter assay and RIP assay. Zhang et al found that miR-501-3p elevated the chemosensitivity of glioma cells to cisplatin through

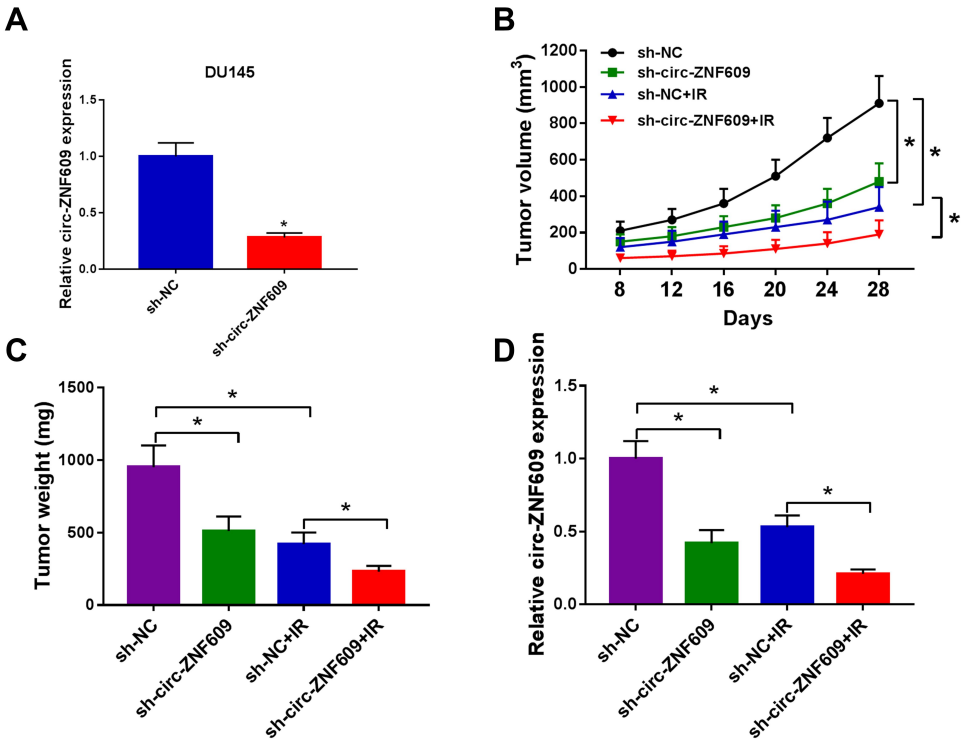

Figure 8 Circ-ZNF609 silencing elevates radiosensitivity of PCa in vivo. (**A**) qRT-PCR was implemented to measure the expression of circ-ZNF609 in DU145 cell line stably transfected with sh-NC or sh-circ-ZNF609. (**B**) Tumor volume in sh-NC group, sh-circ-ZNF609 group, sh-NC + IR group and sh-circ-ZNF609 + IR group was measured every 4 d after 8-d injection. (**C**) Tumors in different groups were resected and weighed after 28-d injection. (**D**) The expression of circ-ZNF609 was detected in different groups by qRT-PCR. *P<0.05.

sponging MYCN.[26] Luo et al claimed that miR-501-3p restrained the motility and development of hepatocellular carcinoma through suppressing LIN7A.[16] MiR-501-3p has been reported to be down-regulated in PCa tissues and cell lines, and the restoration of miR-501-3p level suppressed the proliferation, colony formation and cell cycle of PCa cells through CREPT/cyclin D1 signaling.[17] Consistent with the above article,[17] we found that the level of miR-501-3p was notably decreased in PCa tissues and cell lines. Rescue experiment manifested that circ-ZNF609 promoted the malignant behaviors and radioresistance of PCa cells through targeting and down-regulating miR-501-3p.

HK2 is the first rate-limiting enzyme in the process of glycolysis. The aberrant expression of HK2 was associated with the progression of many cancers. For instance, Tao et al claimed that EZH2 facilitated the progression and glycolysis of PCa through regulating miR-181b/HK2 axis.[27] DeWaal et al demonstrated that the depletion of HK2 suppressed the glycolytic metabolism and promoted the oxidative phosphorylation and chemosensitivity of hepatocellular carcinoma.[28] B7-H3 accelerated the glycolysis and drug resistance of colorectal cancer cells through up-regulating the level of HK2.[29] Furthermore, Fan et al reported that UCA1 enhanced the radioresistance of cervical cancer cells through up-regulating HK2/glycolytic pathway.[30] Here, HK2 was found to be a direct target of miR-501-3p. Further experiments revealed that miR-501-3p exerted a tumor suppressor role in PCa cells through down-regulating HK2.

Through transfecting si-circ-ZNF609 alone or together with anti-miR-501-3p into PCa cells, we found that circ-ZNF609 could up-regulate the abundance of HK2 via sponging miR-501-3p in PCa cells.

Lastly, tumor growth assay was applied to explore the association between the expression of circ-ZNF609 and the radioresistance of PCa cells in vivo. The results revealed that circ-ZNF609 depletion sensitized PCa cells to irradiation in vivo.

Overall, our study demonstrated that circ-ZNF609 promoted the viability, migration and invasion while impeded the apoptosis of PCa cells via miR-501-3p/HK2 axis. Furthermore, circ-ZNF609 also elevated the radioresistance of PCa cells through promoting glycolysis via miR-501-3p/HK2 axis. Our results provided novel potential targets for PCa treatment.

Disclosure

The authors report no funding and no conflicts of interest for this work.

References

1. Prostate cancer. *Aust Nurs Midwifery J*. 2014;22(5):26–28.
2. Hamdy FC, Donovan JL, Lane JA, et al. 10-year outcomes after monitoring, surgery, or radiotherapy for localized prostate cancer. *N Engl J Med*. 2016;375(15):1415–1424. doi:doi:10.1056/NEJMoa1606220
3. Chang AJ, Autio KA, Roach M, Scher HI. High-risk prostate cancer-classification and therapy. *Nat Rev Clin Oncol*. 2014;11(6):308–323. doi:doi:10.1038/nrclinonc.2014.68
4. Hanahan D, Weinberg RA. Hallmarks of cancer: the next generation. *Cell*. 2011;144(5):646–674. doi:10.1016/j.cell.2011.02.013
5. Warburg O. On the origin of cancer cells. *Science*. 1956;123(3191):309–314. doi:10.1126/science.123.3191.309
6. Vander Heiden MG, Cantley LC, Thompson CB. Understanding the Warburg effect: the metabolic requirements of cell proliferation. *Science*. 2009;324(5930):1029–1033. doi:10.1126/science.1160809
7. Kroemer G, Pouyssegur J. Tumor cell metabolism: cancer's Achilles' heel. *Cancer Cell*. 2008;13(6):472–482. doi:doi:10.1016/j.ccr.2008.05.005
8. Vander Heiden MG. Targeting cancer metabolism: a therapeutic window opens. *Nat Rev Drug Discov*. 2011;10(9):671–684. doi:doi:10.1038/nrd3504
9. Chen LL, Yang L. Regulation of circRNA biogenesis. *RNA Biol*. 2015;12(4):381–388. doi:doi:10.1080/15476286.2015.1020271
10. Hamam R, Hamam D, Alsaleh KA, et al. Circulating microRNAs in breast cancer: novel diagnostic and prognostic biomarkers. *Cell Death Dis*. 2017;8(9):e3045. doi:doi:10.1038/cddis.2017.440
11. Jin C, Zhao W, Zhang Z, Liu W. Silencing circular RNA circZNF609 restrains growth, migration and invasion by up-regulating microRNA-186-5p in prostate cancer. *Artif Cells Nanomed Biotechnol*. 2019;47(1):3350–3358. doi:doi:10.1080/21691401.2019.1648281
12. Cai Y, Yu X, Hu S, Yu J. A brief review on the mechanisms of miRNA regulation. *Genomics Proteomics Bioinformatics*. 2009;7(4):147–154. doi:doi:10.1016/s1672-0229(08)60044-3
13. Di Leva G, Garofalo M, Croce CM. MicroRNAs in cancer. *Annu Rev Pathol*. 2014;9:287–314. doi:doi:10.1146/annurev-pathol-012513-104715
14. Acunzo M, Romano G, Wernicke D, Croce CM. MicroRNA and cancer–a brief overview. *Adv Biol Regul*. 2015;57:1–9. doi:doi:10.1016/j.jbior.2014.09.013
15. Lu J, Zhou L, Wu B, et al. MiR-501-3p functions as a tumor suppressor in non-small cell lung cancer by downregulating RAP1A. *Exp Cell Res*. 2020;387(1):111752. doi:doi:10.1016/j.yexcr.2019.111752
16. Luo C, Yin D, Zhan H, et al. microRNA-501-3p suppresses metastasis and progression of hepatocellular carcinoma through targeting LIN7A. *Cell Death Dis*. 2018;9(5):535. doi:doi:10.1038/s41419-018-0577-y
17. Zhang Z, Shao L, Wang Y, Luo X. MicroRNA-501-3p restricts prostate cancer growth through regulating cell cycle-related and expression-elevated protein in tumor/cyclin D1 signaling. *Biochem Biophys Res Commun*. 2019;509(3):746–752. doi:doi:10.1016/j.bbrc.2018.12.176
18. He R, Liu H. TRIM59 knockdown blocks cisplatin resistance in A549/DDP cells through regulating PTEN/AKT/HK2. *Gene*. 2020;747:144553. doi:doi:10.1016/j.gene.2020.144553
19. Cao L, Wang M, Dong Y, et al. Circular RNA circRNF20 promotes breast cancer tumorigenesis and Warburg effect through miR-487a/HIF-1α/HK2. *Cell Death Dis*. 2020;11(2):145. doi:10.1038/s41419-020-2336-0
20. Ameres SL, Zamore PD. Diversifying microRNA sequence and function. *Nat Rev Mol Cell Biol*. 2013;14(8):475–488. doi:10.1038/nrm3611
21. Zhang HD, Jiang LH, Sun DW, Hou JC, Ji ZL. CircRNA: a novel type of biomarker for cancer. *Breast Cancer*. 2018;25(1):1–7. doi:10.1007/s12282-017-0793-9
22. Meng S, Zhou H, Feng Z, et al. CircRNA: functions and properties of a novel potential biomarker for cancer. *Mol Cancer*. 2017;16(1):94. doi:10.1186/s12943-017-0663-2
23. Bi W, Huang J, Nie C, et al. CircRNA circRNA_102171 promotes papillary thyroid cancer progression through modulating CTNNBIP1-dependent activation of β-catenin pathway. *J Exp Clin Cancer Res*. 2018;37(1):275. doi:10.1186/s13046-018-0936-7
24. Zhang Y, Liu H, Li W, et al. CircRNA_100269 is downregulated in gastric cancer and suppresses tumor cell growth by targeting miR-630. *Aging*. 2017;9(6):1585–1594. doi:10.18632/aging.101254
25. Guan Y, Cao Z, Du J, Liu T, Wang T. Circular RNA circPITX1 knockdown inhibits glycolysis to enhance radiosensitivity of glioma cells by miR-329-3p/NEK2 axis. *Cancer Cell Int*. 2020;20:1–13. doi:10.1186/s12935-020-01169-z
26. Zhang CG, Yang F, Li YH, Sun Y, Liu XJ, Wu X. miR-501-3p sensitizes glioma cells to cisplatin by targeting MYCN. *Mol Med Rep*. 2018;18(5):4747–4752. doi:10.3892/mmr.2018.9458
27. Tao T, Chen M, Jiang R, et al. Involvement of EZH2 in aerobic glycolysis of prostate cancer through miR-181b/HK2 axis. *Oncol Rep*. 2017;37(3):1430–1436. doi:10.3892/or.2017.5430
28. DeWaal D, Nogueira V, Terry AR, et al. Hexokinase-2 depletion inhibits glycolysis and induces oxidative phosphorylation in hepatocellular carcinoma and sensitizes to metformin. *Nat Commun*. 2018;9(1):446. doi:10.1038/s41467-017-02733-4
29. Shi T, Ma Y, Cao L, et al. B7-H3 promotes aerobic glycolysis and chemoresistance in colorectal cancer cells by regulating HK2. *Cell Death Dis*. 2019;10(4):308. doi:10.1038/s41419-019-1549-6
30. Fan L, Huang C, Li J, Gao T, Lin Z, Yao T. Long non-coding RNA urothelial cancer associated 1 regulates radioresistance via the hexokinase 2/glycolytic pathway in cervical cancer. *Int J Mol Med*. 2018;42(4):2247–2259. doi:10.3892/ijmm.2018.3778